

## Exploring Galaxy-Halo connection of MW-M31 merged remnant

SWAPNANEEL DEY<sup>1</sup>

<sup>1</sup>*Astronomy Department, University of Arizona*

(Dated: 6th April 2025)

**Keywords:** Dry merger; Dark Matter Halo; Critical Density; R200; Stellar Mass-Halo Mass relation

### 1. INTRODUCTION

Cold dark matter halo potential wells actively drive galaxy formation as they accrete and cool surrounding gas. A **dark matter halo** is the invisible structure of dark matter around a galaxy. This process allows us to predict a strong correlation between galactic properties, such as stellar mass and luminosity, with the halo mass (Girelli et al. 2020). For example, the **stellar-to-halo mass** (SHMR) relation measures the efficiency of a galaxy in converting the mass of its dark matter halo into stars. Since Dark matter halos grow their mass by merging with other such halos, it raises the question of how galaxies and the dark matter halo evolve together through mergers.

It is widely accepted that a significant and ubiquitous process that fuels galaxy evolution is through galaxy mergers. A **galaxy** is a system of stars held together by gravity, whose observed behavior cannot be fully accounted for by ordinary (baryonic) matter and Newtonian gravity alone (Willman & Strader 2012). Most massive galaxies are formed by smaller and other massive galaxies falling into their gravitational potential wells. **Galaxy evolution** is the process by which galaxies grow, morph, and change over time. It is, therefore, imperative to study the evolution of the dark matter halos through the mergers. The results of the study can help constrain various physical processes involved in galaxy mergers, such as feedback mechanisms and how efficiently baryonic matter converts into stars and galaxy assembly.

Though the Halo-Halo merger has been well constrained, the galaxy-galaxy mergers relative to halo-halo mergers remain largely unexplored (Hopkins et al. 2010). Various cosmological hydrodynamical galaxy simulations show that most of the stellar material in massive galaxies is a product of major mergers (merging with a similar massive galaxy) and orbiting satellites (Rodríguez-Gomez et al. 2016). Although there have

been various studies in understanding the merger histories (Fu et al. 2022; Sotillo-Ramos et al. 2022), not much has been done to study the stellar remnant of Milky Way (MW), M31-type galaxies. Figure 1 shows that about 30 percent of simulated MW/M31 type galaxies go through at least one major merger since  $z = 1$  (Sotillo-Ramos et al. 2022). For being so common, it motivates us to understand the Galaxy-Halo connection of stellar remnants of major mergers.

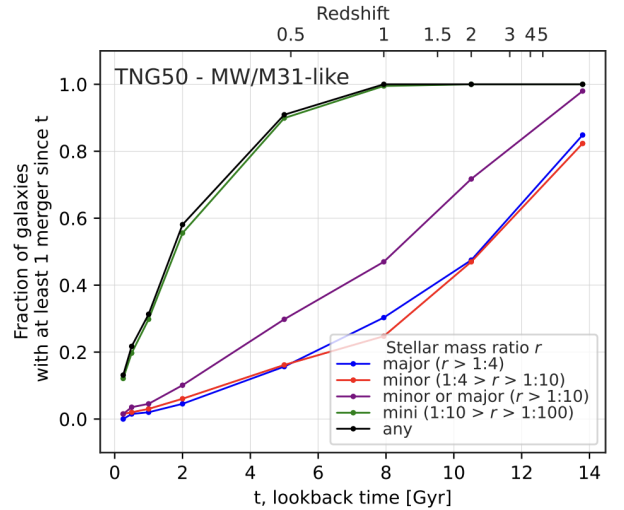


**Figure 1.** Fraction of galaxies with at least one merger versus the lookback time. A major merger, i.e., a merger with a similar massive galaxy, is shown in blue lines. Minor merger, i.e., a merger with a less massive galaxy, is shown in red line, and any merger is shown in black line (Sotillo-Ramos et al. 2022). 30 % of the MW-type galaxies go through a merger.

A leading open question in the Galaxy-Halo connection of stellar remnant is whether the stellar remnant of the merger follows the established SHMR (Moster et al. 2013). The observed burst in star formation in

a merger event may cause a system to deviate from this relation (Hopkins et al. 2010). Or in the case of a **dry merger** (both the colliding systems don't have gas), does the stellar-to-halo mass relation (SHMR) change at different stages of the merger? Furthermore, how long would it take for the merged system to fall back on the relation if there is such a deviation? One kinematics question would be if the angular momentum of the remnant is conserved in a merger event, and what the velocity curve of the remnant halo would look like? Another intriguing question would be whether the phase space diagram of the halo of the remnant looks similar to the phase space diagram of either of the parent galaxies prior to the merger.

## 2. THE PROJECT

This paper will investigate the galaxy-halo connection of the MW-M31 merger's stellar remnant derived from collisionless N-body simulations of the MW and M31 (van der Marel et al. 2012) to see how galaxies and dark matter halos evolve through mergers. Here, N-body simulations simulate how particles like stars and dark matter particles interact with each other under the same physical forces such as gravity.

The main question that this study will answer is whether the stellar remnant follows the established SMHR relation (Moster et al. 2013).

Since MW-M31 is a dry merger, it will be intriguing to see if its remnant deviates from the SMHR. If it does deviate, it could highlight limitations in our current understanding of SMHR and motivate us to have a better relationship. If it lies on the current SMHR, it could motivate understanding how dry mergers without adding new gas or star formation can still follow the relation. This study will help calculate the merger's stellar mass and halo mass and determine its position on SMHR.

## 3. METHODOLOGY

This study uses the N-body simulations of MW and M31 (van der Marel et al. 2012). The model starts with MW at rest at the origin in the galactocentric frame. Galactic disks, each with mass  $M_d$ , were modeled using exponential profiles characterized by a scale length  $R_d$ . The bulges, with mass  $M_b$ , followed the  $R^{1/4}$  profiles. Additionally, a central supermassive black hole with mass  $M_{BH}$  was included in each galaxy. The surrounding dark matter halo was represented using a Hernquist (1990) density profile.

Since the focus is not on mapping the detailed galactic structure of the merger remnant, the analysis relies on low-resolution simulation data. The primary goal is to determine the stellar and halo mass of the merged

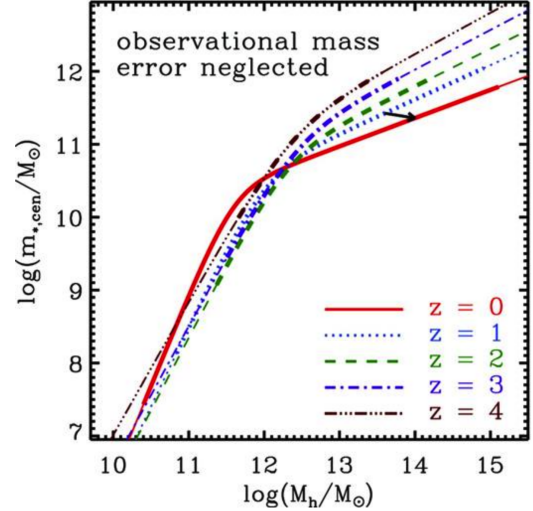


**Figure 2.** Moster relation, Stellar Halo mass relation as a function of halo mass for different redshifts (Moster et al. 2013).

remnant and compare it to the SHMR. The first part of the study would be to establish the SHMR from Moster et al. (2013), as shown in Figure 2, and follows the equation at  $z = 0$ :

$$\frac{m}{M} = 2N \left[ \left( \frac{M}{M_1} \right)^{-\beta} + \left( \frac{M}{M_1} \right)^{\gamma} \right]$$

where,  $m$  = stellar mass,  $M$  = halo mass

$$\log M_1(z) = M_{10} + M_{11} \frac{z}{z+1}; N(z) = N_{10} + N_{11} \frac{z}{z+1}$$

$$\beta(z) = \beta_{10} + \beta_{11} \frac{z}{z+1}; \gamma(z) = \gamma_{10} + \gamma_{11} \frac{z}{z+1}$$

This study uses the exact definition of the parameters as given in Moster et al. (2013), the normalization of the stellar-to-halo mass ratio  $N$ , a characteristic mass  $M_1$  at which  $M/M_1$  equals  $N$ , and two slopes,  $\beta$  and  $\gamma$ , that characterize the slopes of the relation.

The next part of the study is to find the halo and stellar mass of the merger remnant of MW and M31. By creating a function that loops over all the snapshots, we can compute the Center of Mass position and velocity as a function of time. This inherently is the orbit of both galaxies. Here, the Center of mass is computed using the following equation:

$$\mathbf{x}_{COM} = \frac{\sum x_i m_i}{\sum m_i}$$

where  $\mathbf{x}$  is a vector, either position or velocity, and  $m$  is the mass of the particle in the simulation.

We find the epoch when the two systems merge by creating a function that finds the difference between the

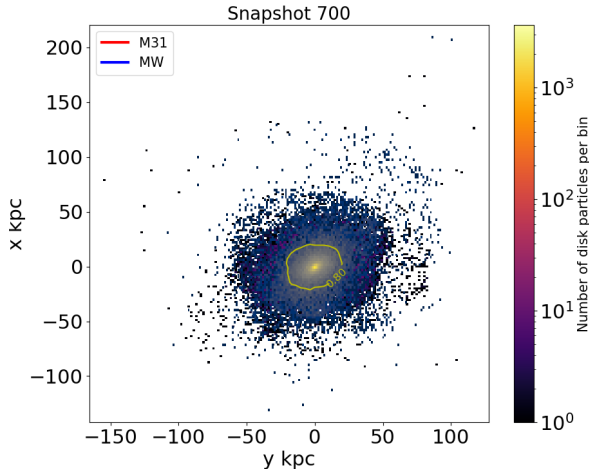


**Figure 3.** Snapshot of when the MW-M31 merger has settled down,  $\sim 10$  Gyr from now. MW particles are shown in blue. M31 particles are the ones in red. 80 % contour level is drawn in yellow.

magnitude of the relative separation and velocity of the two systems. The first merger occurs when the distance between the two COMs is negligible. Any snapshot afterwards, where the merger has settled down, will become our primary data for calculating the remnant’s total stellar and halo mass. For this study, we selected a snapshot of 700, which corresponds to 10 Gyr from now. Figure 3 shows the merged remnant at the chosen time.

We calculate the stellar mass using each galaxy’s disk and bulge particles within the 80 % contour level and the halo mass by using the halo particles within  $r_{200}$  of the merged remnant. Here **R200** is the radius where the average halo density of the merger is equal to  $200 \times$  the critical density of the universe, taken as  $125.6 M_{\odot}/kpc^3$ .

At the end, find the expected stellar mass for the simulated halo mass using the Moster relation defined above. We then compare it to the simulated stellar mass and plot all these values on the SHMR at  $z = 0$  and see how much it deviates. It will also be very intriguing to see how the merger remnant looks on the relationship as it evolves over time.

This study believes that the remnant will not deviate from the SMHR, most likely because it is a dry merger. It does not have enough gas to form new stars; therefore, the merger does not increase the star formation rate.

#### 4. RESULTS

We find the R200 value of the merger to be  $\sim 267$  kpc from the center of mass of the merger. The left plot in Fig. 4 shows the halo density profile of the merge remnant. The right plot overlays the R200 radius in green over the density plot of the merged remnant. De-

Merger	Halo mass	Stellar mass	Stellar mass estimate
Merger	$2.00 \times 10^{12}$	$1.60 \times 10^{11}$	$5.00 \times 10^{10}$
MW	$1.23 \times 10^{12}$	$6.61 \times 10^{10}$	$3.89 \times 10^{10}$
M31	$1.19 \times 10^{12}$	$1.09 \times 10^{11}$	$3.83 \times 10^{10}$

**Table 1.** The halo mass was calculated using R200. The stellar mass in the middle column was calculated using disk+bulge particles within the 80% contour level. The stellar mass estimate was determined using the SMHR of [Moster et al. \(2013\)](#).

spite the very diffuse nature of the halo particles, which spans 1000s of kpcs, the R200, which is used as the defining radius of galaxies, includes about 52% of all the halo particles of the merger. At R200, we get a halo mass of about  $2 \times 10^{12} M_{\odot}$ . Correspondingly, we calculate the stellar mass enclosed within the 80% contour level, as shown in Fig. 3. We find a total stellar mass of  $1.60 \times 10^{11} M_{\odot}$ . Using [Moster et al. \(2013\)](#) equations and our halo mass value, we estimate the required stellar mass of the merger to lie on the SHMR relation. We estimate a value of  $5 \times 10^{10} M_{\odot}$ . Furthermore, for comparison, we follow the same procedure to determine the **current** stellar masses and halo masses, as well as the estimated stellar masses of the Milky Way (MW) and M31. We list these values in table 1.

We plot the values in Table 1 in the Fig. 5. The blue line is the relation established by [Moster et al. \(2013\)](#) for a range of halo masses at  $z = 0$ . Values calculated for the merger, MW, and M31 are displayed in red, black, and green, respectively. The stellar mass calculated from the simulation is shown in a star. The expected stellar mass estimated using the Moster relation at the corresponding halo mass is shown in a circle. The scatter in the relation for  $z = 0$  is shown in gray. We see that both the merger remnant and M31 exhibit stellar masses that lie roughly  $6\sigma$  from the mean scatter, whereas the Milky Way’s stellar mass is only about  $2\sigma$  away.

#### 5. DISCUSSION

One of the main takeaways from Fig. 5 is the huge deviation of the calculated stellar mass from the expected stellar mass. This result doesn’t agree with the hypothesis, which stated that the system would lie within the scatter range of the relation since it’s a dry merger, and that there would be no possibility of forming new stars and temporarily inflating the star formation rate.

This result could be due to a variety of factors. First, it could mean that there is an overestimation of the stellar mass calculated using an 80% confidence level. However, [Moster et al. \(2013\)](#) presents that 80 percent of the stars from the merging galaxies reach the central

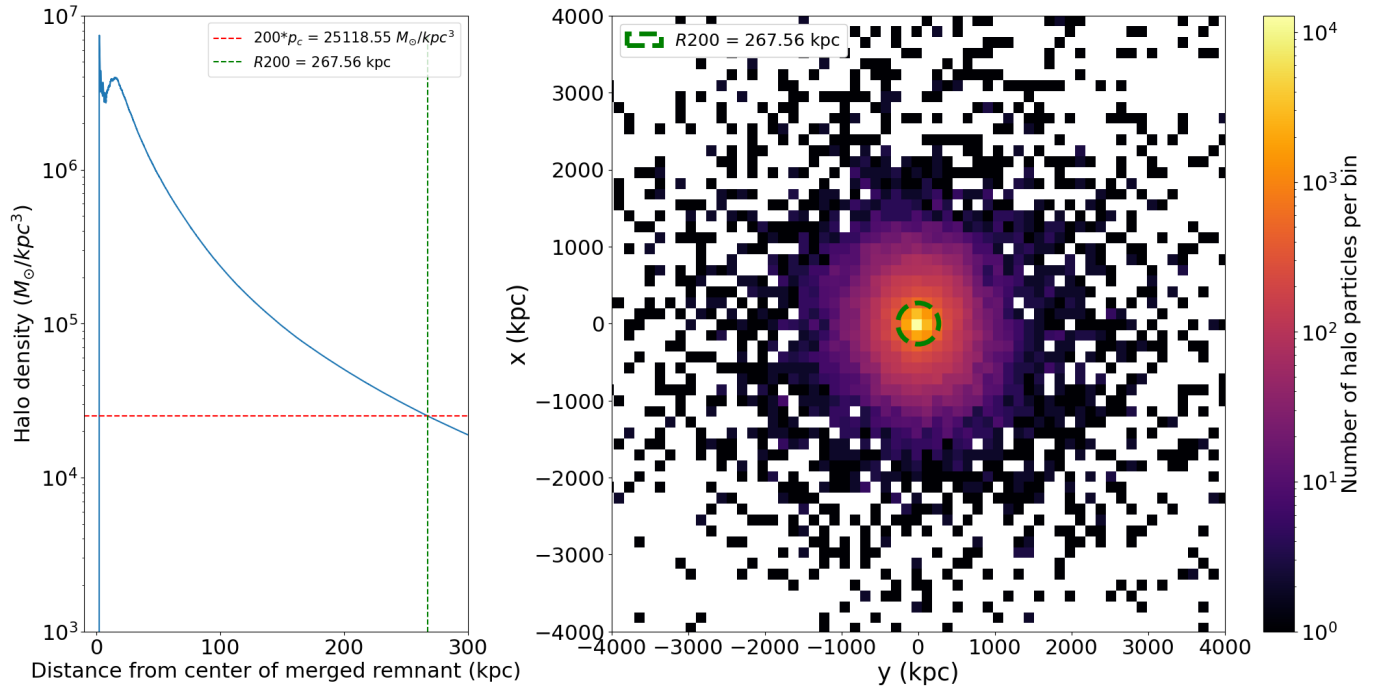


**Figure 4.** Left panel: the halo density profile of the merger remnant. Right panel: the density plot of the merger with the  $R_{200}$  radius indicated in green.

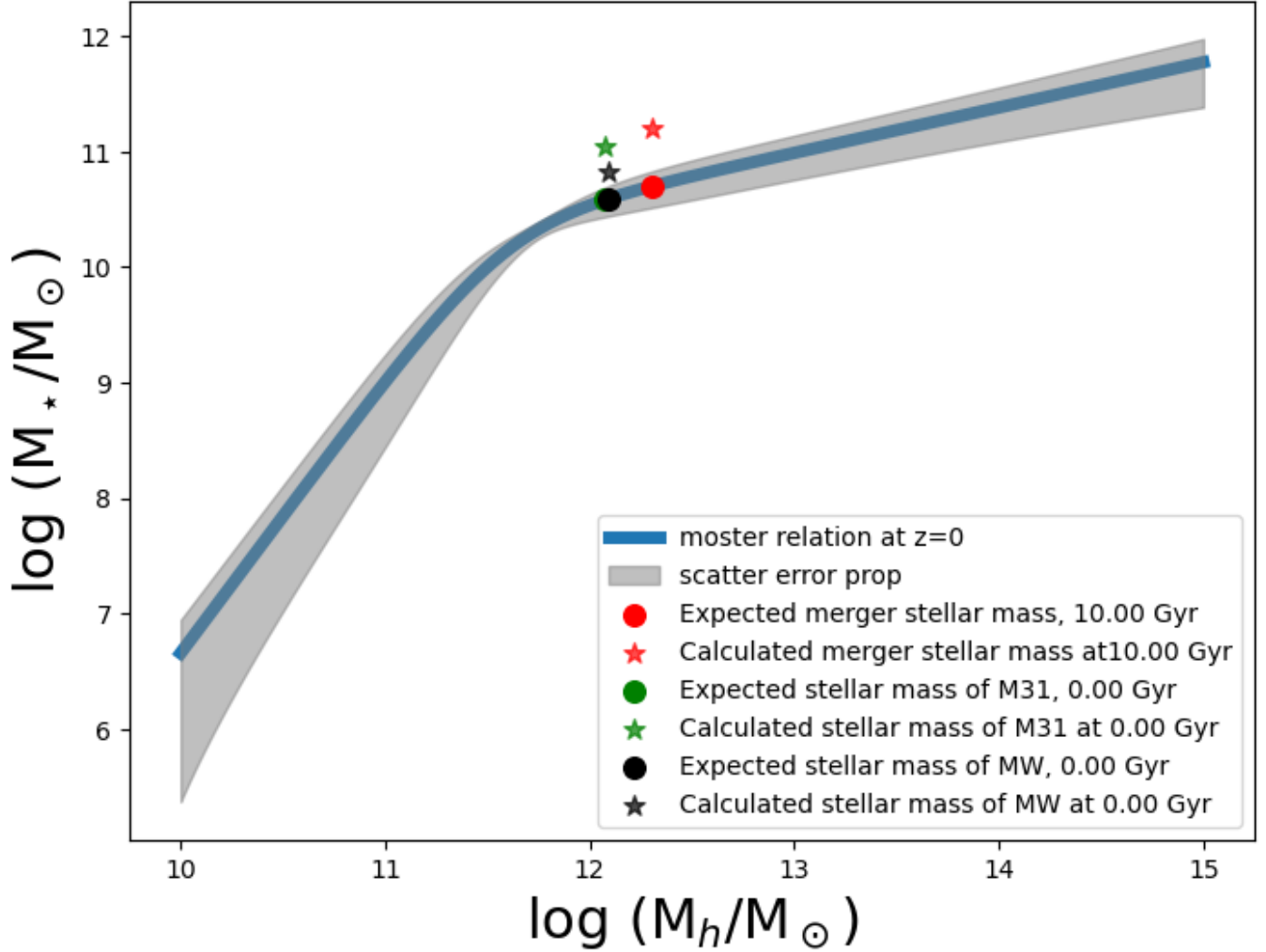


**Figure 5.** SHM relation (Moster et al. 2013) at  $z = 0$ , overlaid with values shown in Table 1. Merger, Milky Way, and M31 values are plotted in red, black, and green, respectively. Simulated stellar masses are marked with stars, while circles denote the stellar masses predicted by the Moster relation at each halo mass. Scatter of the relation is shown in gray.

galaxy. This is also backed up by Behroozi et al. (2013), who find that 70% of the merging stars reach the central galaxy using their model. Secondly, the relation may be more suited to stand-alone galaxies or mergers in a much later stage of their life, where their galactic archaeology has stabilized. The latter does not explain the deviation of the MW, M31 systems, however. Behroozi et al. (2013) has talked about higher efficiency of star formation in halos of masses around  $10^{12} M_\odot$ . This is possibly reflected in our calculation of the stellar mass. Further-

more, simpler functions like the double power law, as used by Moster et al. (2013), can lead to higher uncertainty in the SMF used for fitting the relation at  $z = 0$ . Behroozi et al. (2013) provides a higher number of parameters for fitting the SHMH relation.

The main uncertainties in the studies lie within the error associated with the parameters of the SHM relation used. Furthermore, there may be errors associated with the stellar masses and halo masses calculated from the simulation.

## REFERENCES

- Behroozi, P. S., Wechsler, R. H., & Conroy, C. 2013, *ApJ*, 770, 57, doi: [10.1088/0004-637X/770/1/57](https://doi.org/10.1088/0004-637X/770/1/57)
- Fu, H., Shankar, F., Ayromlou, M., et al. 2022, *MNRAS*, 516, 3206, doi: [10.1093/mnras/stac2205](https://doi.org/10.1093/mnras/stac2205)
- Girelli, G., Pozzetti, L., Bolzonella, M., et al. 2020, *A&A*, 634, A135, doi: [10.1051/0004-6361/201936329](https://doi.org/10.1051/0004-6361/201936329)
- Hernquist, L. 1990, *ApJ*, 356, 359, doi: [10.1086/168845](https://doi.org/10.1086/168845)

- Hopkins, P. F., Bundy, K., Croton, D., et al. 2010, ApJ, 715, 202, doi: [10.1088/0004-637X/715/1/202](https://doi.org/10.1088/0004-637X/715/1/202)
- Moster, B. P., Naab, T., & White, S. D. M. 2013, MNRAS, 428, 3121, doi: [10.1093/mnras/sts261](https://doi.org/10.1093/mnras/sts261)
- Rodriguez-Gomez, V., Pillepich, A., Sales, L. V., et al. 2016, MNRAS, 458, 2371, doi: [10.1093/mnras/stw456](https://doi.org/10.1093/mnras/stw456)
- Sotillo-Ramos, D., Pillepich, A., Donnari, M., et al. 2022, MNRAS, 516, 5404, doi: [10.1093/mnras/stac2586](https://doi.org/10.1093/mnras/stac2586)
- van der Marel, R. P., Besla, G., Cox, T. J., Sohn, S. T., & Anderson, J. 2012, ApJ, 753, 9, doi: [10.1088/0004-637X/753/1/9](https://doi.org/10.1088/0004-637X/753/1/9)
- Willman, B., & Strader, J. 2012, AJ, 144, 76, doi: [10.1088/0004-6256/144/3/76](https://doi.org/10.1088/0004-6256/144/3/76)